Weak antiferromagnetism due to Dzyaloshinskii-Moriya interaction in $Ba_3Cu_2O_4Cl_2$

V. Yushankhai

Max-Planck-Institut für Physik Komplexer Systeme, D-01187 Dresden, Germany
and Joint Institute for Nuclear Research, 141980 Dubna, Russia

M. Wolf, K.-H. Müller, R. Hayn, and H. Rosner

Institut für Festkörper- und Werkstofforschung (IFW) Dresden, D-01171 Dresden, Germany
(Received 5 April 2000)

The antiferromagnetic insulating cuprate $Ba_3Cu_2O_4Cl_2$ contains folded CuO_2 chains with four magnetic copper ions ($S = 1/2$) per unit cell. An underlying multiorbital Hubbard model is formulated and the superexchange theory is developed to derive an effective spin Hamiltonian for this cuprate. The resulting spin Hamiltonian involves a Dzyaloshinskii-Moriya term and a more weak symmetric anisotropic exchange term besides the isotropic exchange interaction. The corresponding Dzyaloshinskii-Moriya vectors of each magnetic Cu-Cu bond in the chain reveal a well defined spatial order. Both, the superexchange theory and the complementary group theoretical consideration, lead to the same conclusion on the character of this order. The analysis of the ground-state magnetic properties of the derived model leads to the prediction of an additional noncollinear modulation of the antiferromagnetic structure. This weak antiferromagnetism is restricted to one of the Cu sublattices.

I. INTRODUCTION

Electronic, superconducting, and magnetic properties of the fast growing family of copper oxides and oxychlorides have attracted much attention in the last years. The undoped parent materials in the cuprate family are insulators showing a variety of low-dimensional magnetic properties. This variety extends from the quasi-two-dimensional (2D) antiferromagnetic (AFM) behavior[1,2] with possible admixture of a weak ferromagnetism[3–7] in the planar compounds to quasi-1D magnetic properties, observable in the chainlike[1,8,9] and spin-ladder[10] systems. The superexchange theory[11–15] provides the necessary basis which allows us to derive and to estimate the main interactions, including anisotropic ones, responsible for the magnetic coupling of the copper spins. The form, and especially the magnitude of several interaction constants of the resulting spin Hamiltonian, however, strongly depend on pecularities of the Cu-O-Cu bond configuration in different cuprates (see Ref. 16 and references therein). One interesting class of magnetic cuprates contains competing magnetic subsystems, like, for instance, tetragonal $Ba_2Cu_3O_4Cl_2$ built up of Cu_3O_4 planes with two types of copper sites (CuI, CuII).[17] It is well known that in $Ba_2Cu_3O_4Cl_2$ (as well as in $Sr_2Cu_3O_4Cl_2$) the moments of the CuI and CuII atoms order antiferromagnetically at different temperatures $T_{N,I} \approx 330–380$ K and $T_{N,II} \approx 30–40$ K, respectively.[4–7,18] Below $T_{N,I}$ a small spontaneous magnetization M_0 within the basal plane of the tetragonal lattice has been reported. The corresponding magnetic structure has been analyzed in Refs. 4–7,18 and 19.

The aim of this paper is to develop the superexchange theory for the orthorhombic compound $Ba_3Cu_2O_4Cl_2$ (space group $Pmma$) with a Cu-O-Cu bond geometry rather unusual in the cuprate family, but having also two crystallographically different types of Cu sites.[20] Actually, in this compound the edge-sharing CuO_4 plaquettes are not aligned

in the same plane, but form folded chains. The chain axis is parallel to the orthorhombic a axis. The unit cell with two sorts, A and B, of crystallographically nonequivalent Cu sites is depicted in Fig. 1. Due to the typical Cu^{2+} ($3d^9$) states the compound is an insulator. It was found to behave like a classical antiferromagnet with a Néel temperature T_N of about 20 K.[7] Below T_N and for applied magnetic fields H_a parallel to the a axis this compound shows a spin-flop transition at $\mu_0 H_a \approx 2.6$ T.[7] Thus the "easy axis" of the antiferromagnetically ordered moments turns out to be the a axis. Above T_N the susceptibility follows a normal Curie-like behavior. From the Curie constant an effective paramagnetic
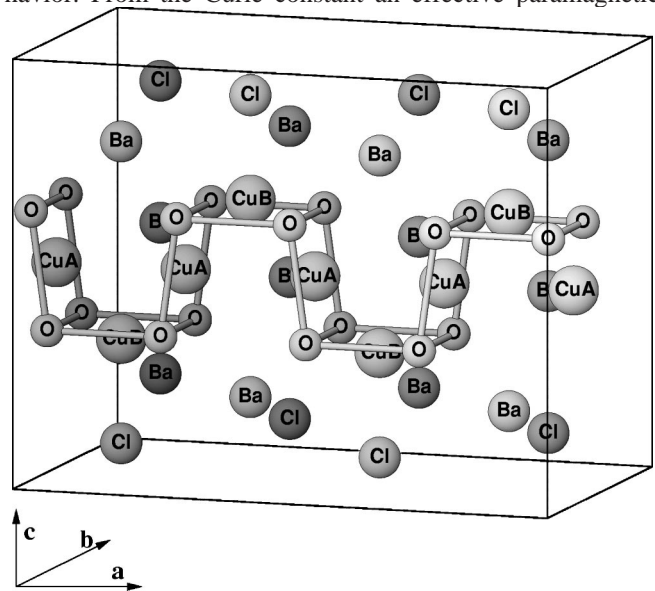

FIG. 1. Two unit cells of $Ba_3Cu_2O_4Cl_2$, space group $Pmma$. The Cu-O_4 plaquettes form folded chains with their axes parallel to the a axis. To better demonstrate one of these CuO_2 chains, the origin in the figure was taken at $(0,1/2,0)$. The crystal structure as well as the chains contain two types of copper sites, Cu_A and Cu_B.

moment of about $2\mu_B$ is derived, which is typical for Cu^{2+} in the $3d^9$ state. No weak ferromagnetism has been observed.[7] Preliminary group theoretical analysis showed[19] that in $Ba_3Cu_2O_4Cl_2$ weak ferromagnetism is forbidden while weak antiferromagnetism cannot be excluded. It is suggesting to explain the expected noncollinearity in the AFM structure due to the presence of Dzyaloshinskii-Moriya -type[21,22] interactions between the Cu spins in $Ba_3Cu_2O_4Cl_2$. Actually, the lack of a center of inversion for each individual Cu-O-Cu bond in a chain clearly shows that such an anisotropic interaction is allowed. However, the space pattern of these local Dzyaloshinskii-Moriya vectors in the entire lattice and its relation to magnetic ground-state peculiarities are far from being obvious. Detailed calculations are necessary to reveal the actual space pattern together with the form of the complete spin Hamiltonian. To solve this problem we develop below a microscopic approach based on the super-exchange theory. The resulting spin model is analyzed to characterize quantitatively the magnetic ground state in $Ba_3Cu_2O_4Cl_2$. In order to remove certain remaining ambiguities the microscopic approach is complemented by symmetry considerations.

The organization of the paper is the following. In the next section the results of the band-structure calculation in the local-density approximation (LDA) for $Ba_3Cu_2O_4Cl_2$ will be briefly presented. The basic set of copper and oxygen orbitals responsible for superexchange processes will be fixed together with the estimates for the corresponding electronic transfer integrals and the orbital crystal-field splitting parameters. At the next step, to provide a background for the superexchange theory the underlying multiorbital Hubbard model is formulated with spin-orbit coupling on copper ions involved. The perturbation expansion of the multiorbital Hubbard model is used in Sec. III to derive an effective spin Hamiltonian for the nearest-neighbor Cu-Cu magnetic interactions. A mean-field analysis of the model derived is also presented and a prediction on the ground-state magnetic structure in $Ba_2Cu_2O_4Cl_2$ is formulated. A complementary group theoretical analysis is presented in Sec. IV. Concluding remarks can be found in Sec. V.

II. BAND STRUCTURE AND THE UNDERLYING MULTIORBITAL HUBBARD MODEL

The band structure of $Ba_3Cu_2O_4Cl_2$ was calculated within the local-density approximation (LDA) using a recently developed full-potential nonorthogonal local-orbital minimum-basis scheme (FPLO).[23] Here, the Cu($3d$, $4s$, $4p$), Ba($5s$, $5p$, $5d$, $6s$, $6p$), Cl($3s$, $3p$, $3d$), and O($2s$, $2p$, $3d$) states were treated as valence states and the lower lying states as core states. For our purpose to extract tight-binding parameters it is sufficient to perform a non-spin-polarized calculation. The nonmagnetic solution shows metallic behavior with four bands crossing the Fermi surface, corresponding to the four copper atoms per unit cell. Hereafter the notations B_1, A_1, B_2, and A_2 will be used to specify the different Cu sites in a unit cell.

Due to the folding of the CuO_2 chains by nearly 90° the bandwidth of the half filled antibonding bands is relatively narrow (≈ 0.5 eV) and only half as large as in the planar (unfolded) edge-shared chains such as in Li_2CuO_2 or

$CuGeO_3$.[24] The orbital analysis for the four bands at Fermi level shows that these bands are built up mainly from the Cu_A-3d_{yz} and the $Cu_B-3d_{x^2-y^2}$ orbitals, respectively, with an admixture of all three $O-2p_x$, $-2p_y$, $-2p_z$ orbitals (the global axes x, y, and z are parallel to the crystallographic a, b, and c axes, respectively). The other Cu–$3d$ orbitals give rise to a band structure (16 bands altogether) which spans the range of binding energies from 2 eV up to 4 eV below the Fermi level. The band states of predominantly O $2p_x$, $2p_y$, $2p_z$ character fall into the range of binding energies from ~ 2 eV up to ~ 6 eV.

The indirect coupling of the Cu–$3d$ orbitals via the intermediate O–$2p$ orbitals can be described by a set of effective hopping matrix elements. Considering first the top-most four bands formed by the active, i.e., spin carrying, Cu_A-3d_{yz} and $Cu_B-3d_{x^2-y^2}$ orbitals we obtained the following results by fitting those bands to a four-band tight-binding (TB) model.[25] The intrachain hopping between the neighboring Cu_A and Cu_B sites, $t_{AB}^x \simeq 65$ meV, is of the same order as the interchain diagonal $Cu_{B_1}-Cu_{B_1}$ hopping, $t_{BB}^{2xy} \simeq -60$ meV. Considering the hierarchy of transfer processes, the next terms were found to be $t_{AA}^y \simeq t_{BB}^y \simeq 30$ meV which correspond to the interchain nearest neighbor hoppings along the y direction. The interlayer hopping parameters along z direction are very weak. Therefore the seemingly quasi-one-dimensional compound $Ba_3Cu_2O_4Cl_2$ has to be classified, in a first approximation, as a two-dimensional compound with spatially anisotropic interactions within a layer and weak couplings between the layers (which are necessary to explain the 3D magnetism and the experimentally found finite Néel temperature). That is true also for the exchange couplings of the spins related to the Cu_A-3d_{xz} and $Cu_B-3d_{x^2-y^2}$ basic orbitals. Below we will consider in great detail the microscopic origin of the dominant intrachain nearest-neighbor interactions that involve rather strong magnetic anisotropies due to the nontrivial geometry of a particular chain. The remaining interchain couplings are expected to influence only the spin isotropic part of the exchange interaction since they occur in a more simple geometry.

To develop the theory of superexchange, in the following the appropriate underlying Hubbard model is formulated for $Ba_3Cu_2O_4Cl_2$. Due to the $S=1/2$ nature of the spins on the Cu^{+2} sites, a single-ion anisotropy cannot occur. A magnetic anisotropy can only be obtained by taking into account simultaneously both, the spin-orbit coupling and the splitting of the orbitals by crystalline fields.[26] The spin-orbit coupling of the copper ions is described by the H_{LS} term in the underlying electronic Hamiltonian. This term and the kinetic one, H_t, are considered as the perturbation while the zero-order Hamiltonian $H_0 = H_0^{(d)} + H_0^{(p)}$ is a sum of the on-site interactions at copper and oxygen atoms, respectively. Thus the complete Hamiltonian is specified as follows:

$$H_0^{(d)} = \sum_j \left\{ \sum_m \sum_\alpha \varepsilon_{jm}^d d_{jm,\alpha}^\dagger d_{jm,\alpha} \right.$$

$$\left. + \sum_{mm'} \sum_{\alpha\alpha'} U_d^{mm'} n_{jm\alpha}^d n_{jm'\alpha'}^d \right\},$$

$$H_0^{(p)} = \sum_l \left\{ \sum_k \sum_\beta \varepsilon_{lk}^p p_{lk,\beta}^\dagger p_{lk,\beta} + \sum_{kk'} \sum_{\beta\beta'} U_p^{kk'} n_{lk\beta}^p n_{lk'\beta'}^p \right\},$$

$$H_t = \sum_{j,m,\alpha} \sum_{l\in j,k} \{t_{jm,lk} d_{jm,\alpha}^\dagger p_{lk,\alpha} + \text{H.c.}\},$$

$$H_{LS} = \lambda \sum_j \vec{L}_j \vec{S}_j, \tag{1}$$

where the hole representation and the standard notation for cuprates are used. Here j, which is a composite index, denotes a cell number and the sort of the Cu site in the cell; $l \in j$ is used to denote an O site neighboring to the j site. The term ε_{jm}^d is the crystal field level for the mth copper d orbital at the jth site. The results of the band structure calculations[25] allow us to estimate the crystal field splitting between the lowest ε_{j0}^d ($=\varepsilon_0^d$) and the excited ($m\neq 0$) levels ε_{jm}^d ($\simeq\varepsilon_m^d$) as $\varepsilon_m^d - \varepsilon_0^d \approx 2\,\text{eV} \equiv \varepsilon_d$. We neglect the difference of this splitting between the different excited m states as well as between the nonequivalent Cu j sites, which is of minor importance for the present purposes. For the further calculations only the copper on-site Coulomb integral $U_d^{mm'}$ with $m'=m$ is required, which is assumed in analogy with other cuprates to be $U_d^{mm} = U_d \simeq 8$–10 eV. The crystal field splitting between the different oxygen $|p_{lk}\rangle$ orbitals ($k=x,y,z$) located on a lattice site l is not taken into account in the present consideration. The estimate for the ''bare'' charge transfer gap $\Delta_p = \varepsilon^p - \varepsilon_0^d \approx 4$ eV is deduced from the band-structure calculations and a complementary finite cluster analysis.[27] For the oxygen on-site Coulomb integrals $U_p^{kk} = U_p$ and $U_p^{kk'} = U_p - 2J_p$ (for $k\neq k'$), the following estimates, $U_p \simeq 4$ eV and $J_p \simeq 0.2$–0.4 eV, standard for the cuprates (see Ref. 28 and references therein), are assumed.

Next, we consider the kinetic part, H_t. According to Slater and Koster (see Ref. 29) one can express the hopping amplitudes $t_{jm,lk}$ between the nearest-neighbor copper $|d_{jm}\rangle$ and oxygen $|p_{lk}\rangle$ orbitals as linear combinations of the two parameters, $(pd\sigma)$ and $(pd\pi)$. By using the approximation $(pd\pi) \simeq -1/2(pd\sigma) = -t_{pd}^{\text{eff}}/\sqrt{3}$ which is valid for transition-metal oxides,[30] one may write $t_{jm,lk} = \chi_{mk} t_{pd}^{\text{eff}}$. In this expression, for given $|d_{jm}\rangle$ and $|p_{lk}\rangle$, the factor χ_{mk} is a function of direction cosines of the $(\vec{j}-\vec{l})$ vector. All these factors, of order unity, are calculated by using the routine procedure.[29] The only parameter remaining, t_{pd}^{eff}, is estimated from the band-structure calculations. For the special composition of CuO$_4$ plaquettes in Ba$_3$Cu$_2$O$_4$Cl$_2$ with only nearest-neighbor Cu-O hopping we obtained the following estimate $t_{pd}^{\text{eff}} \simeq 0.5$ eV by using the formula $t_{AB}^x = (t_{pd}^{\text{eff}})^2/\Delta_p$. That value is smaller than the corresponding nearest-neighbor Cu-O hopping terms in other cuprates[15,28,31,32] since the effects of the different geometry, the neglect of direct O-O transfer, and of the crystal-field splitting at oxygen sites are all condensed into one effective parameter. The value $\lambda = 0.1$ eV of the spin-orbit coupling, characteristic for other cuprates, is taken in the calculation.
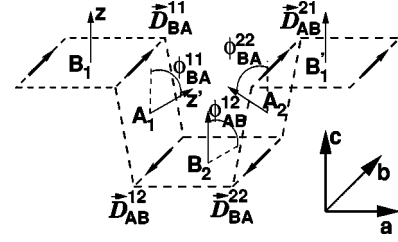

FIG. 2. Spatial ordering of the Dzyaloshinskii-Moriya vectors $\vec{D}_{BA}^{ij}$, etc., related to a pair of Cu atoms located at B_i and A_j. (The first indices refer to the left atom in the pair). The z (z') axes are locally defined and are perpendicular to the corresponding plaquette. The dashed line is the local z (z') axis of the plaquette left to that under consideration and is used for the definition of the angles ϕ_{BA}^{ij}: The rotation of the corresponding dashed line onto the local axis results in the rotation angle ϕ_{BA}^{ij}, the sign of which defines the direction of the local Dzyaloshinskii-Moriya vectors $\vec{D}_{BA}^{ij}$. The crystallographic axes a, b, and c form the global coordinate system.

III. SPIN HAMILTONIAN AND THE MEAN-FIELD GROUND-STATE SPIN CONFIGURATION

The derivation of the effective superexchange interactions using perturbation theory in the multiband Hubbard model, has been presented already many times for planar cuprates.[26,33,34] Some peculiarities of the present derivation are due to the fact that the CuO$_2$ chains in Ba$_3$Cu$_2$O$_4$Cl$_2$ are folded. The unit cell of this structure contains four different Cu ions which are denoted in Fig. 2 as B_1, A_1, B_2, and A_2. Therefore there is a sequence of four different magnetic bonds $(ij) = (B_1,A_1)$, (A_1,B_2), (B_2,A_2), and (A_2,B_1'), where the site B_1' belongs to the neighboring unit cell. We start by deriving the spin Hamiltonian for a particular (AB) or (BA) bond of this sequence, and then extend the consideration to the entire structure. Two oxygen ions, $(l=L,R)$, which are common neighbors of Cu$_A$ and Cu$_B$, mediate the superexchange interaction between Cu$_A$ and Cu$_B$. By applying an appropriate unitary transformation one can define molecular-type basic functions for the oxygen single-hole states in the form $|p_n\rangle = (|p_{Lk}\rangle \pm |p_{Rk}\rangle)/\sqrt{2}$, with ($n = 1, \ldots 6$ for $k=x,y,z$), that are used below.

At the first step of the expansion procedure the excited $|d_{jm}\rangle$ orbitals ($m\neq 0$) are taken into account by additional vector hybrydization terms $\sim\vec{C}_{j,n}\cdot\vec{\sigma}_{\alpha\beta}$ connecting the ground state $|d_{j0}\rangle$ orbitals with different $|p_n\rangle$ orbitals. Then, the original hopping processes $\sim t_{j0,n}$ and the additional new ones can be dealt simultaneously within the same approximation. The corresponding effective kinetic term is

$$H_1^{(AB)} = \sum_{j=A,B} \sum_n \sum_{\alpha\beta} [t_{j0,n}\delta_{\alpha\beta} + \vec{C}_{j,n}\cdot\vec{\sigma}_{\alpha\beta}] d_{j0,\alpha}^\dagger p_{n,\beta} + \text{H.c.}, \tag{2}$$

where $\vec{\sigma}_{\alpha\beta}$ represent the Pauli matrices and

$$\vec{C}_{j,n} = -\frac{\lambda}{2\varepsilon_d} \sum_m \vec{L}_{j,0m} t_{jm,n}; \quad \vec{C}_{n,j}^* = \vec{C}_{j,n}. \tag{3}$$

Here, $\vec{L}_{j,0m}$ are matrix elements of the orbital angular momentum operator and $t_{jm,n}$ are the original amplitudes for the hopping process between the excited mth crystal-field d-state and the nth oxygen p state.

Finally, the $|p_n\rangle$-orbital states can be eliminated in the perturbation procedure and the corresponding fourth-order processes are summed up into the following spin Hamiltonian[33] referring to one Cu_A-(O-O)-Cu_B magnetic bond:

$$H^{(AB)} = J_{AB}\vec{S}_A\vec{S}_B + \vec{D}_{AB}\cdot[\vec{S}_A\times\vec{S}_B] + \vec{S}_A\,\bar{\bar{\Omega}}_{AB}\vec{S}_B \quad (4)$$

with the interaction constants

$$J_{AB} = 4\sum_{nn'} g_{nn'}[t_{A0,n}t_{n,B0} + \vec{C}_{A,n}\cdot\vec{C}_{n,B}]\cdot[t_{B0,n'}t_{n',A0}$$
$$+ \vec{C}_{B,n'}\cdot\vec{C}_{n',A}],$$

$$\vec{D}_{AB} = 8\iota\sum_{nn'} g_{nn'}t_{A0,n}t_{n,B0}[\vec{C}_{B,n'}t_{n',A0} + t_{B0,n'}\vec{C}_{n',A}],$$

$$\Omega_{AB}^{\mu\nu} = \Gamma_{AB}^{\mu\nu} + \Gamma_{AB}^{\nu\mu} - \delta_{\mu\nu}\left(\sum_{\xi}\Gamma_{AB}^{\xi\xi}\right), \quad (5)$$

$$\Gamma_{AB}^{\mu\nu} = 4\sum_{nn'} g_{nn'}[C_{A,n}^{\mu}t_{n,B0} + t_{A0,n}C_{n,B}^{\mu}]\cdot[C_{B,n'}^{\nu}t_{n',A0}$$
$$+ t_{B0,n'}C_{n',A}^{\nu}].$$

Here $g_{nn'}$ is given by

$$g_{nn'} = \frac{1}{\Delta_p^2}\left[\frac{1}{U_d} + \frac{1}{2\Delta_p} + \frac{1}{2\Delta_p + U_p^{nn'}}\right], \quad (6)$$

where $U_p^{nn} = U_p$ and $U_p^{nn'} = U_p - 2J_p$ ($n' \neq n$). Further on the notation $g_{nn} = g$ will be used. One may note a weak difference between g_{nn} ($n' = n$) and $g_{nn'}$ ($n' \neq n$). Taking into account the particular form of the $t_{j0,n}$ ($= t_{n,j0}$) and $\vec{C}_{j,n}$ ($= \vec{C}_{n,j}^*$) transfer parameters, we find the final expressions for the nonzero interaction constants:

$$J_{AB} = 4gb_{AB}^2 - \delta J_{AB},$$

$$D_{AB}^y = 8gb_{AB}c_{AB}, \quad (7)$$

$$\Gamma_{AB}^{yy} = 4gc_{AB}^2 - \delta\Gamma_{AB}^{yy},$$

where

$$b_{AB} = (t_{pd}^{\text{eff}})^2(1 - \cos\phi_{AB}),$$

$$c_{AB} = \frac{1}{\sqrt{3}}\left(\frac{\lambda}{\varepsilon_d}\right)(t_{pd}^{\text{eff}})^2\sin\phi_{AB},$$

$$\delta J_{AB} \approx \left(\frac{\lambda}{\varepsilon_d}\right)^2 4gb_{AB}^2, \quad (8)$$

$$\delta\Gamma_{AB}^{yy} \approx \left(\frac{J_p}{2\Delta_p + U_p}\right)4gc_{AB}^2.$$

It is worth emphasizing at this stage that the vector $\vec{D}_{AB}$ of the Dzyaloshinskii-Moriya interaction is directed along the $\vec{y}$ axis (i.e., $D_{AB}^x = D_{AB}^z = 0$) and the symmetric anisotropy is described by only one nonzero parameter Γ_{AB}^{yy}. Note that the direction of $\vec{D}_{AB}$ is in agreement with the rules given by Moriya.[22] The parameter ϕ_{AB} is characteristic for the directed (AB) bond. More generally, a particular parameter ϕ_{ij} has to be assigned to each bond in the entire chainlike structure in the following way. Let us ascribe to the center of each jth plaquette a local $\vec{z}_j$ axis perpendicular to the plane of the plaquette. For instance, in Fig. 2 the $\vec{z}(=\vec{z}_i)$ and $\vec{z}'$ ($=\vec{z}_j$) are related to $i = B_1$ and $j = A_1$, respectively. Then, ϕ_{ij} is the angle of the rotation which transforms the local $\vec{z}_i$ axis into the $\vec{z}_j$ axis. Therefore one has

$$\phi_{BA}^{11} = -\phi_{AB}^{12} = -\phi_{BA}^{22} = \phi_{AB'}^{21} \simeq 84°, \quad (9)$$

where the left (right) indices refer to the left (right) atom in the directed bond. It can be directly checked that each magnetic bond is described by the same form of the spin Hamiltonian (4)–(8). By using the relations (7–9) it can be easily seen that the parameters J and Γ^{yy} are bond independent while the component D_{ij}^y changes the sign in accordance with Eq. (9). The spin Hamiltonian for the entire chainlike magnetic system can be written in the following form:

$$\mathcal{H} = \sum_{ij}\mathcal{H}^{(ij)}, \quad \mathcal{H}^{(ij)} = \mathcal{H}_0^{(ij)} + \delta\mathcal{H}^{(ij)},$$

$$\mathcal{H}_0^{(ij)} = 4g\{b^2\vec{S}_i\cdot\vec{S}_j + 2bc\xi_{ij}\vec{d}\cdot[\vec{S}_i\times\vec{S}_j]$$
$$+ c^2[2(\vec{d}\vec{S}_i)(\vec{d}\vec{S}_j) - \vec{S}_i\cdot\vec{S}_j]\},$$

$$\delta\mathcal{H}^{(ij)} = -\delta J\vec{S}_i\vec{S}_j - \delta\Gamma^{yy}[2(\vec{d}\vec{S}_i)(\vec{d}\vec{S}_j) - \vec{S}_i\vec{S}_j], \quad (10)$$

where $\vec{d}$ is the unit vector along the global $\vec{b}$ axis. $\xi_{ij} = \text{sgn}\phi_{ij}$ determines the space pattern of the Dzyaloshinskii-Moriya vectors for the chainlike structure [see Eq. (9)].

Below the arguments given by Shekhtman, Entin-Wohlman, and Aharony[35] for the single-bond superexchange interactions are extended to the chainlike magnetic system with this special pattern of the $\vec{D}_{ij}$ vectors. Actually, the spins in the lattice can be subdivided into two subsystems in such a way that the first (second) subsystem is formed by the spins in B (A) positions only. Let us now introduce the following redefinition of the spin variables:

$$\tilde{\vec{S}}_{B_1} = \vec{S}_{B_1}, \quad \tilde{\vec{S}}_{B_2} = \vec{S}_{B_2},$$

$$\tilde{\vec{S}}_{A_1} = (\vec{d}\cdot\vec{S}_{A_1})\vec{d} + \cos\theta[\vec{S}_{A_1} - (\vec{d}\cdot\vec{S}_{A_1})\vec{d}] - k\sin\theta[\vec{S}_{A_1}\times\vec{d}], \quad (11)$$

$$\tilde{\vec{S}}_{A_2} = (\vec{d}\cdot\vec{S}_{A_2})\vec{d} + \cos\theta[\vec{S}_{A_2} - (\vec{d}\cdot\vec{S}_{A_2})\vec{d}] + k\sin\theta[\vec{S}_{A_2}\times\vec{d}],$$

where $k=\pm 1$ and $k\tan\theta=-2bc/(b^2-c^2)$. It should be noted, that the transformation (11) corresponds to a rotation of the spins $\vec{S}_{A_1}$ ($\vec{S}_{A_2}$) by an angle θ ($-\theta$) with $\vec{d}$ as the rotation axis. The Hamiltonian $\mathcal{H}_0^{(ij)}$ is strictly transformed into an isotropic form[35] while concerning the remaining $\delta\mathcal{H}^{(ij)}$ an additional justification should be made. Actually, no terms higher than of second order in (λ/ε_d) have been kept up to now. By noting that $\delta J,\delta\Gamma\sim(\lambda/\varepsilon_d)^2$ and in Eq. (11) the angle $\theta\sim(\lambda/\varepsilon_d)$, the consistent way is to keep the form of $\delta\mathcal{H}^{(ij)}$ but using the transformed spin variables. Finally the transformed Hamiltonian $\tilde{\mathcal{H}}=\Sigma\tilde{\mathcal{H}}^{(ij)}$ takes the form

$$\tilde{\mathcal{H}}^{(ij)}=\bar{J}\tilde{\vec{S}}_i\tilde{\vec{S}}_j-\bar{\Gamma}\{2(\vec{d}\tilde{\vec{S}}_i)(\vec{d}\tilde{\vec{S}}_j)-(\tilde{\vec{S}}_i\cdot\tilde{\vec{S}}_j)\} \quad (12)$$

with the renormalized constants $\bar{J}=4g(b^2+c^2)-\delta J$, and $\bar{\Gamma}=\delta\Gamma^{yy}>0$.

A mean-field analysis of this Hamiltonian shows that the expected classical ground-state configuration is a collinear antiferromagnetic array of the transformed spins (11) in the magnetically easy xz plane, $\bar{\Gamma}>0$. We emphasize that according to Eq. (12) the staggered moment is not confined to a particular direction in the easy xz plane. This "residual" symmetry of the derived superexchange can be broken by additional interaction terms not included into the consideration up to now. Postponing a discussion of possible sources for additional anisotropies let us now assume that the residual symmetry is broken in such a way that the staggered magnetization is parallel to the $\vec{x}$ axis (i.e., crystallographic a direction), and in the ground state the spins $\tilde{\vec{S}}_{B_1}$ ($=\vec{S}_{B_1}$) and $\tilde{\vec{S}}_{B_2}$ ($=\vec{S}_{B_2}$) are aligned in the $\vec{x}$ direction. This is supported by the symmetry analysis of the following Section, which demands that the staggered magnetization $\vec{L}=(\vec{M}_{A_1}+\vec{M}_{A_2}-\vec{M}_{B_1}-\vec{M}_{B_2})/2$ has to be parallel to one of the crystallographic axis. In the mean-field approximation one may immediately write

$$\tilde{\vec{S}}_{B_1}=-\tilde{\vec{S}}_{A_1}=\tilde{\vec{S}}_{B_2}=-\tilde{\vec{S}}_{A_2}=S\vec{e}_x \quad (13)$$

and performing the inverse transformation one obtains for the original spins

$$\vec{S}_{B_1}=\vec{S}_{B_2}=S\vec{e}_x,$$

$$\vec{S}_{A_1}=-S[\cos\theta\cdot\vec{e}_x+k\sin\theta\cdot\vec{e}_z], \quad (14)$$

$$\vec{S}_{A_2}=-S[\cos\theta\cdot\vec{e}_x-k\sin\theta\cdot\vec{e}_z].$$

The corresponding picture for the double degenerate classical ground-state spin configuration is given in Fig. 3. A weak transverse (along the $\vec{z}$ axis) modulation in the second sublattice is imposed on the strong antiferromagnetic correlations between the spins belonging to different sublattices. This weak antiferromagnetic modulation is entirely due to the Dzyaloshinskii-Moriya interaction. The angle θ for this modulation is estimated to be
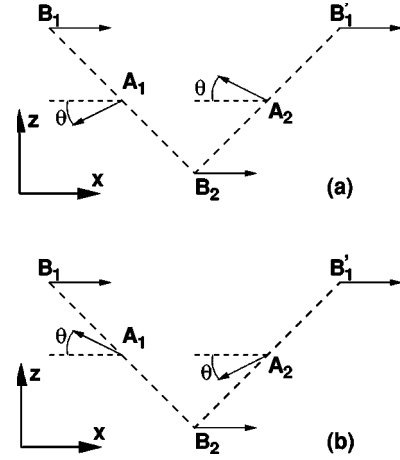
FIG. 3. Within a classical picture (mean-field approximation) the Dzyaloshinskii-Moriya interaction between the magnetic moments (arrows) of the Cu_A and Cu_B atoms results in a small canting of the Cu_A moments (canting angle $\pm\theta$). The ground state is twofold degenerated (a,b) and reveals weak antiferromagnetism. The two states differ by the sign of the canting angle and the direction of the additional antiferromagnetic vector $L_{A,z}=M_{A1,z}-M_{A2,z}$ of the Cu_A sublattice. x and z are global axes equivalent to the crystallographic a and c axes.

$$\theta\simeq\frac{|\vec{D}_{ij}|}{J}\simeq\frac{2c}{b}=\frac{2}{\sqrt{3}}\left(\frac{\lambda}{\varepsilon_d}\right)|\sin\phi_{ij}|\simeq3^\circ. \quad (15)$$

with an absolute value of $|\vec{D}_{ij}|\sim0.25$ meV corresponding to $J\sim5$ meV. It is worth mentioning that the magnetization measurements[7] for $Ba_3Cu_2O_4Cl_2$ have clearly shown that the crystallographic a direction ($\vec{x}$ axis in our notations) is the preferred direction for the staggered moment below T_N, where $T_N\simeq20$ K is the temperature of the three-dimensional antiferromagnetic ordering. According to this analysis it is expected that the ground state in this compound is not a simple collinear antiferromagnetic configuration, but involves also a weak antiferromagnetic superstructure due to the Dzyaloshinskii-Moriya interaction.

To our knowledge, in cuprates only weak ferromagnetism (WFM) was reported up to now. The corresponding spin canting angle, which measures the deviation from collinearity, is rather small, $\theta_{WFM}\simeq0.05^\circ$ (compare for instance Refs. 3,26,33 and 34). In the present case the spin canting angle (15), i.e., $\theta\simeq3^\circ$, is more than an order of magnitude larger. The reason for this difference is the following. Although the spin-orbit coupling $(\lambda/\varepsilon_d)\sim0.1$ is nearly the same in both cases, the geometrical factor is much larger in the present case as $|\sin\phi_{ij}|\simeq1$ due to the strong folding of the chains ($|\phi_{ij}|\simeq84^\circ$).

It is necessary to discuss the possible influence of transverse interchain magnetic interactions to show the validity of the derived spin anisotropy. We assume that the dominant interaction between two neighboring spins belonging to different chains in a layer is the isotropic superexchange with an AFM interaction constant $J_\perp$. By using the results of the band-structure calculations (Sec. II) we found the estimate $J_\perp/J\sim0.25$, where J is the intrachain exchange constant. Due to the presence of the center of inversion for the transverse Cu-Cu magnetic bond a Dzyaloshinskii-Moriya term

FIG. 4. Symmetry elements of a Cu_A-Cu_B chain in $Ba_3Cu_2O_4Cl_2$. The magnetic moments are located at the $2c$ sites (A_1, A_2, and A_1') and at the $2e$ sites (B_1, B_2 and B_1'). The symmetry elements mapping the chain onto itself are: axes C_{2z} going through the B sites, axes C_{2y} (sketched by small ellipses) perpendicular to the x-z plane and going through the A sites, and inversion centers located at the sites A_i.

cannot occur and the symmetric anisotropy is expected to be very weak. The band-structure results indicate also a weak interlayer exchange $J_z \ll J_\perp, J$ and more distant interchain Cu-Cu exchange interactions (for instance, to third neighbors in the plane of Cu_B). However, the spin anisotropy of the latter interaction is expected to be small due to the planar geometry of the corresponding exchange path.

IV. SYMMETRY AND SPATIAL ORDERING OF THE DZYALOSHINSKII-MORIYA VECTORS

In order to derive the spatial order of the Dzyaloshinskii-Moriya vectors by symmetry considerations, at first the symmetry analysis of the antiferromagnetic states in $Ba_3Cu_2O_4Cl_2$ (following Refs. 36–38), presented elsewhere,[19] will be summarized. It is assumed that the lattice constant a of the magnetic unit cell and that of the crystallographic unit cell are identical. As has been pointed out in Ref. 38 it is sufficient to consider the independent symmetry

operations. For the space group $Pmma$ besides the identity there are only three independent symmetry elements.

A very convenient choice for these elements is: rotation axis C_{2y} through the point ($x_0 = 0$, $z_0 = 1/2$), rotation axis C_{2z} through the point ($x_0 = 1/4$, $y_0 = 0$) and inversion I located at ($x_0 = 0$, $y_0 = 0$, $z_0 = 1/2$). As these elements map a given chain onto itself no assumptions concerning the relative orientation of moments in different chains are necessary. The magnetic moments reside on the $2c$ sites Cu_{A1}, Cu_{A2}, and $Cu_{A'1}$, and on the $2e$ sites Cu_{B1}, Cu_{B2}, and $Cu_{B'1}$ (see Fig. 4, in which also the mentioned symmetry elements are sketched). Obviously the ion Cu_{A1} (Cu_{B1}) is equivalent to $Cu_{A'1}$ ($Cu_{B'1}$). Because the sites of the $2c$ and $2e$ sublattices are crystallographically not equivalent, the magnetic order has to be characterized by two antiferromagnetic (AFM) vectors,

$$\vec{L}_A = \vec{M}_{A1} - \vec{M}_{A2}, \quad \vec{L}_B = \vec{M}_{B1} - \vec{M}_{B2}, \quad (16)$$

and two sublattice magnetizations,

$$\vec{m}_A = (\vec{M}_{A1} + \vec{M}_{A2})/2, \quad \vec{m}_B = (\vec{M}_{B1} + \vec{M}_{B2})/2, \quad (17)$$

where $\vec{M}_{Ai}$ ($\vec{M}_{Bj}$) are the magnetic moments of the Cu_{Ai} (Cu_{Bj}) ions at the sites A_i (B_j). The interchange of the moments $\vec{M}_i \leftrightarrow \vec{M}_j$ generated by the symmetry operations is given in the second and third column of Table I. As only one ordering temperature is found, both AFM vectors have to transform according to the same magnetic group, compatible with the crystallographic space group $Pmma$. The transformation behavior for each component $L_{A,x}$, $L_{A,y}$, etc. and for the sublattice magnetizations $\vec{m}_A$ and $\vec{m}_B$ is described in Table I by two numbers characterizing two steps of the corresponding transformation: the transformation of $\vec{L}_A$, $\vec{L}_B$, etc. due to $\vec{M}_i \leftrightarrow \vec{M}_j$ (first number) and the remaining part of the transformation (rotation, inversion; second). The entry $+1$ means no change of the considered vector component, -1 means a change of sign. In the line below the resulting magnetic symmetry element is given. As $I\vec{L}_A = \vec{L}_A$, but $RI\vec{L}_B = \vec{L}_B$ the AFM vectors $\vec{L}_{2c}$ and $\vec{L}_{2e}$ cannot simulta-

TABLE I. The first column lists the independent symmetry elements of the space group $Pmma$, here chosen to be E, C_{2z}, C_{2y} and I. The second and third columns give the magnetic moments $\vec{M}_{Ai}$ and $\vec{M}_{Bj}$ ($i, j = 1, 2$) generated from $\vec{M}_{A1}$ and $\vec{M}_{B1}$ by applying these symmetry elements. In the remaining columns for each component of the antiferromagnetic vectors $\vec{L}_A = \vec{M}_{A1} - \vec{M}_{A2}$, $\vec{L}_B = \vec{M}_{B1} - \vec{M}_{B2}$, and the two sublattice magnetizations $\vec{m}_A = (\vec{M}_{A1} + \vec{M}_{A2})/2$ and $\vec{m}_B = (\vec{M}_{B1} + \vec{M}_{B2})/2$ two numbers are given: the first takes into account the interchange $\vec{M}_{A1} \leftrightarrow \vec{M}_{A2}$, $\vec{M}_{B1} \leftrightarrow \vec{M}_{B2}$ ($1 \leftrightarrow$ no change of the vector components, $-1 \leftrightarrow$ vector components change sign). The second $+1$ or -1 describes the remaining part of the considered transfomation (rotation, inversion). The resulting magnetic group elements are given in the line below these two numbers (R: time reversal).

	$\vec{M}_{Ai}$	$\vec{M}_{Bj}$	$L_{A,x}$	$L_{A,y}$	$L_{A,z}$	$L_{B,x}$	$L_{B,y}$	$L_{B,z}$	$m_{A,x}$ $m_{B,x}$	$m_{A,y}$ $m_{B,y}$	$m_{A,z}$ $m_{B,z}$
E	$\vec{M}_{A1}$ ($2c$ site)	$\vec{M}_{B1}$ ($2e$ site)									
C_{2z}	$\vec{M}_{A2}$	$\vec{M}_{B1}$	-1,-1 C_{2z}	-1,-1 C_{2z}	-1,1 RC_{2z}	1,-1 RC_{2z}	1,-1 RC_{2z}	1,1 C_{2z}	1,-1 RC_{2z}	1,-1 RC_{2z}	1,1 C_{2z}
C_{2y}	$\vec{M}_{A1}$	$\vec{M}_{B2}$	1,-1 RC_{2y}	1,1 C_{2y}	1,-1 RC_{2y}	-1,-1 C_{2y}	-1,1 RC_{2y}	-1,-1 C_{2y}	1,-1 RC_{2y}	1,1 C_{2y}	1,-1 RC_{2y}
I	$\vec{M}_{A1}$	$\vec{M}_{B2}$	1,1 I	1,1 I	1,1 I	-1,1 RI	-1,1 RI	-1,1 RI	1,1 I	1,1 I	1,1 I

neously become different from zero. As each component of $\vec{m}_A$ and $\vec{m}_B$ transforms according to the same magnetic group, the only possibility for antiferromagnetic ordering is $L_x = m_{A,x} - m_{B,x} \neq 0$, $L_y = m_{A,y} - m_{B,y} \neq 0$ or $L_z = m_{A,z} - m_{B,z} \neq 0$. This means that ferromagnetic order is predicted for each of the two crystallographic Cu sublattices. The moments of the crystallographically different sublattices are antiparallel to each other. As different components of $\vec{m}_A$ and $\vec{m}_B$ belong to different magnetic groups (Table I) (i) only one component of the AFM vector $\vec{L}$ may be different from zero, i.e., $\vec{L}$ is parallel to one of the crystallographic axes, and (ii) weak ferromagnetism is excluded, contrary to the case of $Ba_2Cu_3O_4Cl_2$. This is in agreement with the experiments. The symmetry analysis cannot predict the direction of the AFM vector. Experiments show $L_x \neq 0$.[7] For that case, independent magnetic symmetry elements are E, RC_{2z}, RC_{2y}, and I. Interestingly, Table I shows, that for that case a small $L_{A,z} \neq 0$, i.e., weak antiferromagnetism[36] can additionally occur.

As shown in Sec. III, within the unit cell this weak antiferromagnetism is described by a sum of Dzyaloshinskii-Moriya terms

$$
\begin{aligned}
H_{WAFM} = {} & D_{BA}^{11} \cdot (M_{B1,x}M_{A1,z} - M_{B1,z}M_{A1,x}) \\
& + D_{AB}^{12} \cdot (M_{A1,x}M_{B2,z} - M_{A1,z}M_{B2,x}) \\
& + D_{BA}^{22} \cdot (M_{B2,x}M_{A2,z} - M_{B2,z}M_{A2,x}) \\
& + D_{AB'}^{21} \cdot (M_{A2,x}M_{B'1,z} - M_{A2,z}M_{B'1,x}). \quad (18)
\end{aligned}
$$

This interaction has to be invariant with respect to the symmetry operations RC_{2z}, RC_{2y}, and I. Using the transformation properties of the moments according to Table I, the equivalence of sites differing by a lattice translation along the a axis, results in

$$
D_{BA}^{11} = -D_{AB}^{12} = -D_{BA}^{22} = D_{AB'}^{21}. \quad (19)
$$

As to be expected, the spatial order of the local Dzyaloshinskii-Moriya vectors determined from the symmetry of the magnetic unit cell is the same as that derived by analyzing the relations between the different bonds in the previous section. Moreover, the symmetry analysis together with the experimental results shows, that in the transformation described in Sec. III (canting of the moments) the Cu_{Bi} moments have to be fixed, as L_B has to remain zero for an AFM state with moments parallel to the a axis.

V. CONCLUSIONS

The superexchange interaction between two neighboring but crystallographically nonequivalent Cu ions in $Ba_3Cu_2O_4Cl_2$ was analyzed within a multiorbital Hubbard model. This superexchange interaction was expressed by an effective spin-spin Hamiltonian. As there is no center of inversion for the considered Cu-(O-O)-Cu entity, this interaction involves the Dzyaloshinskii-Moriya term, which refers to the corresponding bond. By means of an analysis of the geometric relations between neighboring bonds (plaquettes) the spatial order of these locally defined Dzyaloshinskii-Moriya vectors was determined. This spatial order was also derived by a symmetry analysis taking into account the experimentally found ''easy axis'' of the staggered magnetization. These considerations revealed, that spin canting occurs in the subsystem of the Cu_A magnetic moments only. Within the presented microscopic model, for the magnetic moments all directions within the a-c plane are equivalent. The anisotropy, leading to the experimentally observed spin-flop transition for applied fields parallel to the a axis could not yet be explained. Further investigations have to be done to find the microscopic origin for additional anisotropies, which break the easy-plane symmetry of the superexchange model and explain the experimentally observed easy-axis behavior. With this respect, two main contributions have been ignored in the considered Hamiltonian (1). First of all, the theory of superexchange can be developed at a more sophisticated level by adopting more details of the electronic structure of the real compound. For instance, the form of the symmetric anisotropy tensor is rather sensitive to an actual crystal-field splitting of p orbitals on oxygen ions. This splitting should be taken into account into the theoretical scheme. A second reason leading to a breakdown of the easy-plane symmetry involves the direct-exchange contribution[39] to the symmetric anisotropy term. This is due to the exchange part of the two-site Coulomb multiorbital d-d correlations which should be also incorporated into the Hamiltonian (1). However, for such calculations reliable quantitative estimates for the parameters are required (i.e., the crystal-field states of the O ions and the two-site exchange Coulomb integrals of Cu ions). Since the direct exchange contribution can be hardly obtained within the LDA band-structure analysis, we have to leave this problem for future investigations. From an experimentally point of view, the detection of the discussed weak antiferromagnetism is a challenging task.

[1] D.C. Johnston, in *Handbook of Magnetic Materials*, edited by K.H.J. Buschow (North-Holland, Amsterdam, 1997), Vol. 10, p. 1.

[2] M. Greven, R.J. Birgeneau, Y. Endoh, M.A. Kastner, M. Matsuda, and G. Shirane, Z. Phys. B **96**, 465 (1995).

[3] T. Thio, T.R. Thurster, N.W. Preyer, P.J. Picone, M.A. Kastner, H.P. Jenssen, D.R. Gabbe, C.Y. Chen, R.J. Birgeneau, and A. Aharony, Phys. Rev. B **38**, 905 (1988); K. Fukuda, S. Shamoto, M. Sato, and K. Oka, Solid State Commun. **65**, 1323 (1988).

[4] T. Ito, H. Yamaguchi, and K. Oka, Phys. Rev. B **55**, R684 (1997).

[5] F.C. Chou, Amnon Aharony, R.J. Birgeneau, O. Entin-Wohlman, M. Greven, A.B. Harris, M.A. Kastner, Y.J. Kim, D.S. Klein-

berg, Y.S. Lee, and Q. Zhu, Phys. Rev. Lett. **78**, 535 (1997).

[6] M.A. Kastner, Amnon Aharony, R.J. Birgeneau, F.C. Chou, O. Entin-Wohlman, M. Greven, A.B. Harris, Y.J. Kim, Y.S. Lee, M. E. Parks, and Q. Zhu, Phys. Rev. B **59**, 14 702 (1999).

[7] D. Eckert, K. Ruck, M. Wolf, G. Krabbes, and K.-H. Müller, J. Appl. Phys. **83**, 7240 (1998).

[8] M. Matsuda, K. Katsumata, K.M. Kojima, M. Larkin, G.M. Luke, J. Merrin, B. Nachumi, Y.J. Uemura, H. Eisaki, N. Motoyama, S. Uchida, and G. Shirane, Phys. Rev. B **55**, R11 953 (1997).

[9] M. Troyer, M.E. Zhitomirsky, and K. Ueda, Phys. Rev. B **55**, R6117 (1997).

[10] E. Dagotto and T.M. Rice, Science **271**, 618 (1996).

[11] P.W. Anderson, Phys. Rev. **115**, 2 (1959); Solid State Phys. **14**, 99 (1963).

[12] J. Goodenough, *Magnetism and the Chemical Bond* (John Wiley and Sons, New York, 1963).

[13] T. Moriya, Phys. Rev. Lett. **4**, 228 (1960); Phys. Rev. **120**, 91 (1960).

[14] W. Geertsma, Physica B **164**, 241 (1990).

[15] H. Eskes and J. Jefferson, Phys. Rev. B **48**, 9788 (1993).

[16] A. Aharony, O. Entin-Wohlman, and A.B. Harris, in *Dynamical Properties of Unconventional Magnetic Systems*, edited by A.T. Skjeltorp and D. Sherrington (Kluwer Academic, Dordrecht, 1998).

[17] R. Kipka and Hk. Müller-Buschbaum, Z. Anorg. Allg. Chem. **419**, 58 (1976).

[18] K. Yamada, N. Suzuki, and Y. Akimitsu, Physica B **213&214**, 191 (1995).

[19] K.-H. Müller and M. Wolf, J. Appl. Phys. **87**, 6022 (2000).

[20] R. Kipka and Hk. Müller-Buschbaum, Z. Anorg. Allg. Chem. **422**, 231 (1976).

[21] I.J. Dzyaloshinskii, Phys. Chem. Solids **4**, 241 (1958).

[22] T. Moriya, in *Magnetism* edited by G.T. Rado and H. Suhl (Academic Press, New York, 1963), Vol. I.

[23] K. Koepernik and H. Eschrig, Phys. Rev. B **59**, 1743 (1999).

[24] H. Rosner, R. Hayn, and S.L. Drechsler, Physica B **259-261**, 1001 (1999).

[25] H. Rosner, R. Hayn, S.L. Drechsler, K. Koepernik, and H. Eschrig (unpublished).

[26] D. Coffey, T.M. Rice, and F.C. Zhang, Phys. Rev. B **44**, 10 112 (1991).

[27] L. Siurakshina and V. Yushankhai, Physica B **259-261**, 487 (1999).

[28] V. Yushankhai and R. Hayn, Europhys. Lett. **47**, 116 (1999).

[29] W.A. Harrison, *Electronic Structure and the Properties of Solids* (Dover, New York, 1989), p. 480.

[30] L.F. Mattheiss, Phys. Rev. B **5**, 290 (1972).

[31] L.F. Mattheiss and D.R. Hamann, Phys. Rev. B **40**, 2217 (1989).

[32] H. Rosner, R. Hayn, and J. Schulenburg, Phys. Rev. B **57**, 13 660 (1998).

[33] W. Koshibae, Y. Ohta, and S. Maekawa, Phys. Rev. B **47**, 3391 (1993).

[34] W. Koshibae, Y. Ohta, and S. Maekawa, Phys. Rev. B **50**, 3767 (1994).

[35] L. Shekhtman, O. Entin-Wohlman, and A. Aharony, Phys. Rev. Lett. **69**, 836 (1992).

[36] E.A. Turov, *Physical Properties of Magnetically Ordered Crystals* (Academic Press, New York, 1965).

[37] A.S. Borovik-Romanov, in *Elements of Theoretical Magnetism*, edited by S. Krupicka and J. Sternbeck (Academia, Prague, 1968).

[38] E.F. Bertaut, in *Magnetism*, edited by G.T. Rado and H. Suhl (Academic Press, New York, 1963), Vol. III.

[39] L. Shekhtman, A. Aharony, and O. Entin-Wohlman, Phys. Rev. B **47**, 174 (1993).